

All-Electron Density Functional Study on Electronic Structure, Stability, and Ni–Ni Bonding in Polynuclear Nickel Complexes with Bridging Alkyne Ligands

Jonas Koch,[†] Isabella Hyla-Kryspin,[†] Rolf Gleiter,^{*,†} Thomas Klettke,[‡] and Dirk Walther[‡]

Organisch-Chemisches Institut der Universität Heidelberg, Im Neuenheimer Feld 270, D-69120 Heidelberg, Germany, and Institut für Anorganische und Analytische Chemie der Universität Jena, August-Bebel-Strasse 2, D-07743 Jena, Germany

Received April 20, 1999

The method of density functional theory (DFT) has been used to study chain propagation reactions of zerovalent nickel complexes containing acetylene and σ -donor ligands. The calculations were carried out with all-electron basis sets of triple- ξ quality for the valence region and augmented with polarization functions. Gradient-optimized structures are compared with known experimental data. Stationary points on the potential energy surfaces are characterized by means of calculated vibrational analyses. Computed energetics of the aggregation reaction $L_2Ni(C_2H_2) + L'_2Ni(C_2H_2) \rightarrow L_2Ni(C_2H_2)NiL'_2 + C_2H_2$ ($2L = C_2H_2$, $L' = NH_3$ (**2a**); $2L = Ni(C_2H_2)_2$, $2L' = C_2H_2$ (**3a**); $2L = 2L' = C_2H_2$ (**7**); $2L = C_2H_2$, $2L' =$ none (**10**); $L = L' = PH_3$ (**11**), CO (**12**), none (**13**)) together with results of natural bond orbital (NBO) population analyses are used in the discussion of metal–metal bonding and the thermodynamic stability of acetylene-bridged polynuclear Ni(0) compounds. Ni–Ni interactions in **2a**, **3a**, **7**, and **11–13** are compared with those in the hypothetical molecule $[NiL_2]_2$ ($L = PH_3$ (**9**), $2L = C_2H_2$ (**10**)) as well as with the d^9 – d^9 system of the existing $(\mu-C_2H_2)[Ni(C_5H_5)]_2$ (**8**).

Introduction

In recent synthetic and structural studies on homoleptic complexes of Ni(0) with a variety of alkyne ligands carried out in the laboratory of one of the present authors it was found that complexes of this type could only be isolated and crystallographically characterized when one of the substituents, R' , contained an OH group.¹ Chart 1 depicts some typical examples.

Intermolecular hydrogen bonds between OH groups of neighboring molecules gave rise to a supramolecular structure of complex **1** in the solid state. In the solution at room temperature only mononuclear **1** was present. Below $-15^\circ C$, however, an aggregation to form the trinuclear complex **3** occurred¹ (eq 1).



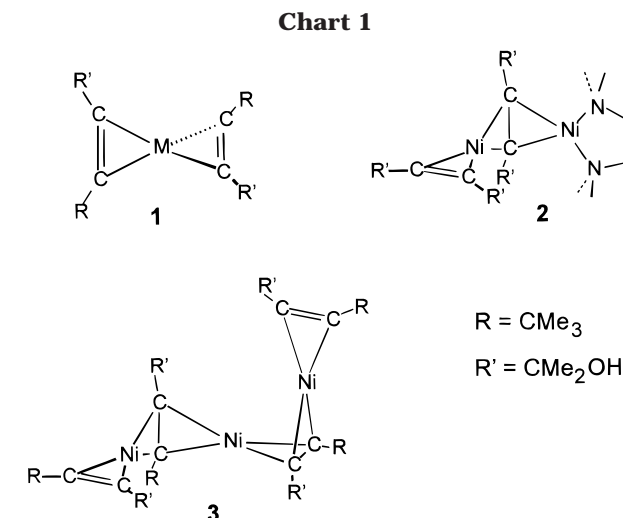
Complex **3** was the third member of the homologous series $M_n(RC\equiv CR')_{n+1}$ ($M = d^{10}$ metal) to be crystallographically characterized.^{1b} So far members with $n = 1$ are known for $M = Ni$,^{1a,c} Pt ,² Cu^+ ³ and compounds

[†] Universität Heidelberg.

[‡] Universität Jena.

(1) (a) Walther, D.; Schmidt, A.; Klettke, T.; Imhof, W.; Görls, H. *Angew. Chem.* **1994**, *106*, 1421; *Angew. Chem., Int. Ed. Engl.* **1994**, *33*, 1373. (b) Walther, D.; Klettke, T.; Görls, H. *Angew. Chem.* **1995**, *107*, 2022; *Angew. Chem., Int. Ed. Engl.* **1995**, *34*, 1860. (c) Walther, D.; Klettke, T.; Schmidt, A. *Organometallics* **1996**, *15*, 2314.

(2) (a) Dubey, R. J. *Acta Crystallogr.* **1975**, *B31*, 1860. (b) Green, M.; Grove, D. M.; Howard, J. A. K.; Spencer, J. L.; Stone, F. G. A. *J. Chem. Soc., Chem. Commun.* **1976**, 759. (c) Boag, N. M.; Green, M.; Grove, D. M.; Howard, J. A. K.; Spencer, J. L.; Stone, F. G. A. *J. Chem. Soc., Dalton Trans.* **1980**, 2170.

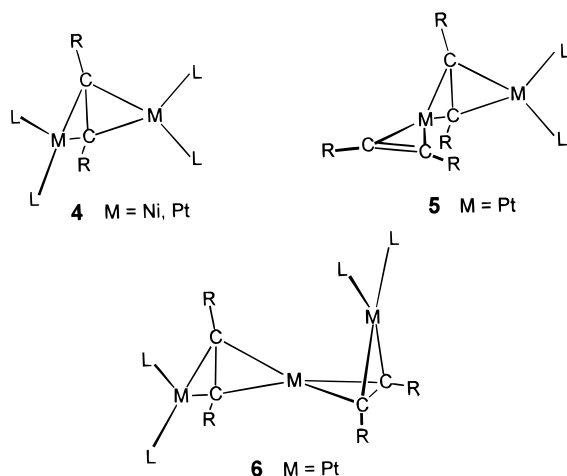


with $n = 2$ have been spectroscopically detected for $M = Pt$.⁴ According to X-ray investigations of **3** hydrogen bonds between OH substituents of the alkyne ligands are of both inter- and intramolecular nature.^{1b} In general $M_n(RC\equiv CR')_{n+1}$ species can be regarded as condensation products of mononuclear complexes with one bridging alkyne replacing two terminal ones. If the aggregation process involves only the $M_n(RC\equiv CR')_{n+1}$ species, there is a potential for further condensation,

(3) Carriedo, G. A.; Miguel, D.; Riera, V.; Solans, X.; Font-Altaba, M.; Coll, M. *J. Organomet. Chem.* **1986**, *299*, C43.

(4) Boag, N. M.; Green, M.; Howard, J. A. K.; Stone, F. G. A.; Wade, H. J. *J. Chem. Soc., Dalton Trans.* **1981**, 862.

Chart 2



i.e., for the formation of homoleptic chains. However, condensation of a $M(RC\equiv CR)L_2$ ($L = \sigma$ -donor ligand) molecule with mono- or polynuclear alkyne complexes introduces a chain-terminating ML_2 unit. Experimentally characterized complexes of this type are schematically displayed in Chart 2.⁵

As condensation occurs by replacement of two terminal alkynes by one bridging alkyne, the corresponding equilibrium presumably does not favor chain propagation. Some additional driving forces such as intramolecular hydrogen bonds or some kind of metal–metal bonding should be present for chain propagation to occur spontaneously. To investigate the question of such stabilizations of complexes **2** and **3**, we have carried out density functional studies on the model compounds $Ni_2(C_2H_2)_2(NH_3)_2$ (**2a**), $Ni_3(C_2H_2)_4$ (**3a**), and $Ni_2(C_2H_2)_3$ (**7**). Since an analysis of the bonding between two or more d^{10} metal centers is not an easy task, for reasons of comparison we have included in our investigations two additional compounds, the acetylene-bridged d^9 – d^9 system $[(C_5H_5)Ni]_2(C_2H_2)$ (**8**)⁶ and the purely hypothetical d^{10} – d^{10} clusters $[NiL_2]_2$ ($L = PH_3$ (**9**), $2L = C_2H_2$ (**10**)), which lack any bridging acetylene ligand. Although two closed-shell metal atoms are normally expected to repel each other, the evidence for a weak bond between two d^{10} metals is well-established from experimental and theoretical studies, especially in the case of gold(I) compounds.^{7,8} The presence of d^{10} – d^{10} interactions in gold(I) compounds has been attributed to the relativistic effect that results in the contraction of the 6s orbital and the expansion of the 5d orbitals.⁹

(5) (a) Day, V. W.; Abdel-Meguid, S. S.; Dabestani, S.; Thomas, M. G.; Pretzer, W. R.; Muetterties, E. L. *J. Am. Chem. Soc.* **1976**, *98*, 8289. (b) Muetterties, E. L.; Pretzer, W. R.; Thomas, M. G.; Beier, B. F.; Thorn, D. L.; Day, V. W.; Anderson, A. B. *J. Am. Chem. Soc.* **1978**, *100*, 2090. (c) Boag, N. M.; Green, M.; Howard, J. A. K.; Spencer, J. L.; Stansfield, R. F. D.; Thomas, M. D. O.; Stone, F. G. A.; Woodward, P. J. *J. Chem. Soc., Dalton Trans.* **1980**, 2182. (d) See also: Bonrath, W.; Pörschke, K. R.; Wilke, G.; Angermund, K.; Krüger, C. *Angew. Chem.* **1988**, *100*, 853; *Angew. Chem., Int. Ed. Engl.* **1988**, *27*, 833.

(6) (a) Mills, O. S.; Shaw, B. W. *J. Organomet. Chem.* **1968**, *11*, 595. (b) Wang, Y.; Coppens, P. *Inorg. Chem.* **1976**, *15*, 1122. (c) See also: Anderson, A. B. *J. Am. Chem. Soc.* **1978**, *100*, 1153.

(7) (a) Schmidbaur, H.; Graf, W.; Müller, G. *Angew. Chem.* **1988**, *100*, 439; *Angew. Chem., Int. Ed. Engl.* **1988**, *27*, 417. (b) Schmidbaur, H. *Gold Bull.* **1990**, *23*, 11. (c) Narayanaswamy, R.; Young, M. A.; Parkhurst, E.; Oullette, M.; Kerr, M. E.; Ho, F. M.; Elder, R. C.; Bruce, A. E.; Bruce, M. R. M. *Inorg. Chem.* **1993**, *32*, 2506. (d) Harwell, D. E.; Mortimer, M. D.; Knobler, C. B.; Anet, F. A. L.; Hawthorn, M. F. *J. Am. Chem. Soc.* **1996**, *118*, 2679. (e) Tang, S. S.; Chang, C.-P.; Lin, I. B. J.; Liou, L.-S.; Wang, J.-C. *Inorg. Chem.* **1997**, *36*, 2294.

Since in the case of the first-row transition metals relativistic effects are by far less important,¹⁰ these effects should not much affect the chemistry of these compounds. In a previous paper we discussed the factors governing the molecular geometry of polynuclear alkyne complexes of d^{10} metals.¹¹ The present studies focus on the thermodynamics of the aggregation process and on the role of Ni–Ni bonding.

Computational Details

For DFT¹² calculations we have used the local density correlation potential by Vosko et al.¹³ and Becke's three-parameter functional¹⁴ with nonlocal correlation corrections of Lee, Yang, and Parr,¹⁵ known in the literature by its acronym B3LYP. Geometry optimizations were carried out with the gradient technique. Vibrational frequencies were obtained from analytical calculations of the Hessian matrixes. The description of the bonding situation has been carried out by means of the natural bond orbital (NBO) method.¹⁶ In this approach the computed electron density is expressed by occupation numbers n_i ($0 \leq n_i \leq 2$) of localized NBOs that match well with the one-center ("lone-pair") and two-center ("bond") elements of the classical Lewis structure of the molecule. The stabilization energy associated with electron delocalizations from donor NBO(i) having occupation values near two electrons into the empty or only slightly populated non-Lewis orbitals, NBO(j), is calculated by means of second-order perturbation theory (eq 2).

$$E_{ij}^{(2)} = n_i F_{ij}^2 / (\epsilon_j - \epsilon_i) \quad (2)$$

In eq 2 n_i is the donor orbital occupancy, ϵ_i and ϵ_j are the diagonal elements (NBO energies), and F_{ij} is the off-diagonal element of the Fock matrix in the NBO basis. A single all-electron basis set was applied in our studies. The Ni atom was described by a Wachters (14s,9p,5d) basis set¹⁷ and augmented with a 4f polarization function ($\alpha_f = 1.29$). The contraction scheme was [9s,5p,3d,1f]. The basis set of McLean and Chandler¹⁸ was used for P, and for C, N, and H the 6-311G basis was adopted.¹⁹ The basis sets of the heavy atoms were augmented by a single 3d polarization function ($\alpha_P = 0.55$; $\alpha_C = 0.626$; $\alpha_N = 0.913$). The calculations were carried out with the Gaussian94 package of programs.²⁰

Results and Discussion

A. Optimized Structures of $(C_2H_2)Ni(\mu-C_2H_2)Ni(NH_3)_2$ (**2a**), $(C_2H_2)Ni(\mu-C_2H_2)Ni(\mu-C_2H_2)Ni(C_2H_2)$

(8) (a) Görling, A.; Rösch, N.; Ellis, D. E.; Schmidbaur, H. *Inorg. Chem.* **1991**, *30*, 3986. (b) Häberlen, O. D.; Schmidbaur, H.; Rösch, N. *J. Am. Chem. Soc.* **1994**, *116*, 8241. (c) Pyykkö, P. *Chem. Rev.* **1997**, *97*, 597. (d) Pyykkö, P.; Runeberg, N.; Mendizabal, F. *Chem. Eur. J.* **1997**, *3*, 1451. (e) Pyykkö, P.; Mendizabal, F. *Chem. Eur. J.* **1997**, *3*, 1458. (f) Pyykkö, P.; Mendizabal, F. *Inorg. Chem.* **1998**, *37*, 3018.

(9) (a) Pyykkö, P.; Desclaux, J. P. *Acc. Chem. Res.* **1979**, *12*, 276. (b) Pitzer, K. S.; *Acc. Chem. Res.* **1979**, *12*, 271. (c) Pyykkö, P. *Chem. Rev.* **1988**, *88*, 563.

(10) Kaltsoyannis, N. *J. Chem. Soc., Dalton Trans.* **1997**, 1. (11) Hyla-Kryspin, I.; Koch, J.; Gleiter, R.; Klettke, T.; Walther, D. *Organometallics* **1998**, *21*, 4724.

(12) (a) Kohn, W.; Sham, L. J. *Phys. Rev. A* **1965**, *140*, 1133. (b) Parr, R. G.; Yang, W. *Density Functional Theory of Atoms and Molecules*; Oxford University Press: Oxford, U.K., 1989.

(13) Vosko, S. H.; Wilk, L.; Nusair, M. *Can. J. Phys.* **1980**, *58*, 1200. (14) Becke, A. D. *J. Chem. Phys.* **1992**, *96*, 2155; **1993**, *98*, 5648.

(15) (a) Lee, C.; Yang, W.; Parr, R. G. *Phys. Rev. B* **1988**, *37*, 785. (b) Miehlich, B.; Savin, A.; Stoll, H.; Preuss, H. *Chem. Phys. Lett.* **1989**, *157*, 200.

(16) (a) Foster, J. P.; Weinhold, F. *J. Am. Chem. Soc.* **1980**, *102*, 7211. (b) Reed, A. E.; Weinhold, F. *J. Chem. Phys.* **1983**, *78*, 4066. (c) Reed, A. E.; Weinstock, R. B.; Weinhold, F. *J. Chem. Phys.* **1985**, *83*, 735. (d) Reed, A. E.; Curtiss, L. A.; Weinhold, F. *Chem. Rev.* **1988**, *88*, 899.

(17) Wachters, A. J. H. *J. Chem. Phys.* **1970**, *52*, 1033. (18) McLean, A. D.; Chandler, G. S. *J. Chem. Phys.* **1980**, *72*, 5639. (19) Krishnan, R.; Binkley, J. S.; Seeger, R.; Pople, J. A. *J. Chem. Phys.* **1980**, *72*, 650.

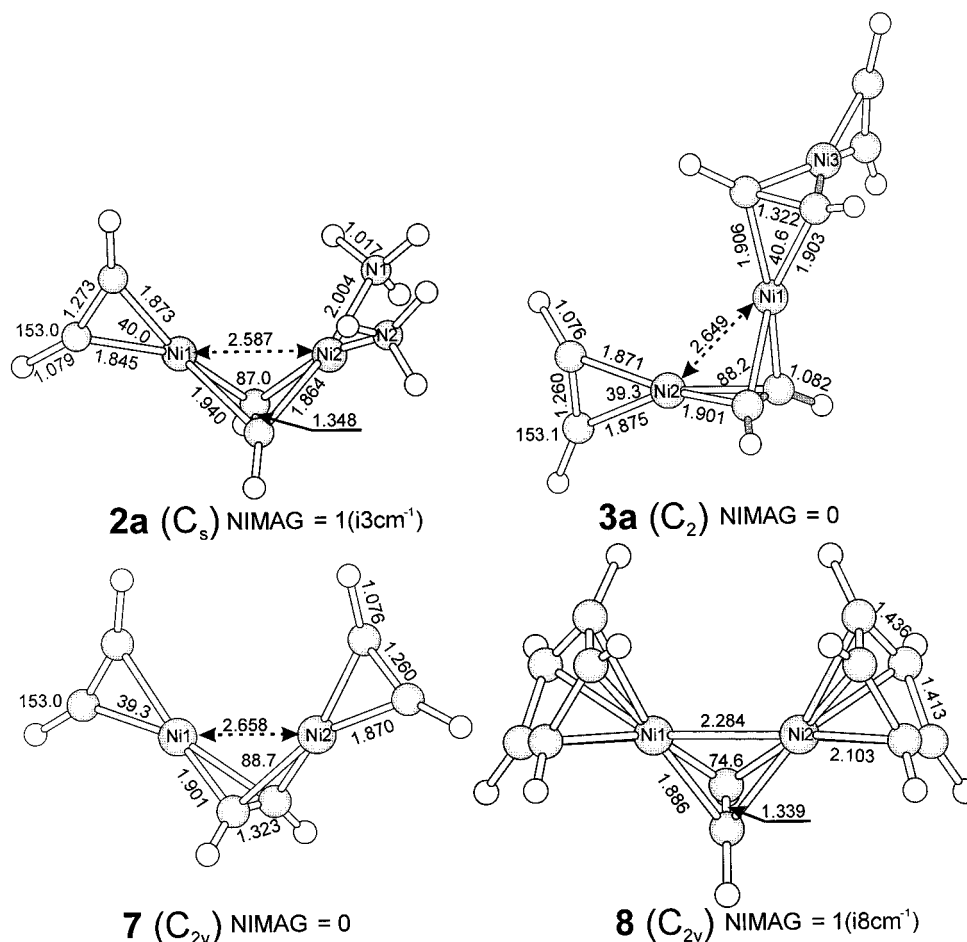


Figure 1. Optimized geometrical parameters and number of imaginary frequencies (NIMAG) of **2a**, **3a**, **7**, and **8**. Bond distances are given in Å and bond angles in deg.

(3a), $(C_2H_2)Ni(\mu-C_2H_2)Ni(C_2H_2)$ (**7**), and $(C_5H_5)Ni(\mu-C_2H_2)Ni(C_5H_5)$ (**8**). The geometry optimizations for **2a**, **3a**, **7**, and **8** were carried out under C_s , C_2 , C_{2v} , and C_{2v} symmetry constraints, respectively. The corresponding gradient-optimized structures are shown in Figure 1. The optimized structures of **3a** and **7** are calculated to be true minima on the potential energy surface. For **2a** and **8** the vibrational analysis shows one imaginary mode which corresponds to the respective rotation of the NH_3 and C_5H_5 ligands. The frequencies $i3\text{ cm}^{-1}$ (**2a**) and $i8\text{ cm}^{-1}$ (**8**) are extremely small and indicate that a very small rotation should lead to the adjacent minimum. Since such a small structural change certainly will not affect the wave function or the energy, we did not further explore the rotation of the ligands. In Table 1 we compare the calculated structural parameters of **2a**, **3a**, and **8** with experimental values.

With the exception of the Ni–Ni distance and the N–Ni–N bond angle of **2a** the agreement between theory and experiment is very good. We ascribe the smaller N–Ni–N angle of 87.3° in the TMED ligand of **2** compared with 99.8° for two NH_3 ligands in **2a** to

Table 1. Geometrical Parameters of **2a**, **3a**, and **8**^a

	2a		3a		8	
	calcd	exptl ^b	calcd	exptl ^c	calcd	exptl ^d
Ni1–Ni2/3	2.588	2.449	2.649	2.547; 2.568	2.284	2.345
Ni2–N1	2.004	2.035				
Ni2–N2	2.004	2.042				
Ni1–C ^b	1.940	1.938	1.903	1.917; 1.927	1.886	1.884
	1.940	1.968	1.906	1.975; 1.965		
Ni2/3–C ^b	1.864	1.879	1.900	1.887; 1.889	1.886	1.884
	1.864	1.907	1.901	1.958; 1.941		
Ni–C ^t	1.873	1.876	1.871	1.879; 1.883		
	1.845	1.847	1.875	1.889; 1.892		
C ^t –C ^t	1.273	1.268	1.260	1.259; 1.250		
C ^b –C ^b	1.348	1.344	1.322	1.323; 1.320	1.339	1.341
$\angle\text{Ni1–Ni2–Ni2}$	99.8	87.3				
$\angle\text{Ct–Ni–Ct}$	40.0	39.8	39.3	39.0		
$\angle\text{Cb–Ni1–Cb}$	40.7	40.2	40.6	39.6	41.6	41.7
$\angle\text{Cb–Ni2–Cb}$	44.8	41.6	40.7	40.1	41.6	41.7

^a Bond distances are given in Å and bond angles in deg. ^b Reference 1a. ^c Reference 1b. ^d Reference 6b.

steric constraints in the chelate. The optimized Ni–Ni distances of **2a** and **3a** are 0.139 \AA (**2a**) and $0.081/0.102\text{ \AA}$ (**3a**) longer than the experimental values of complexes **2** and **3**, respectively. In contrast, the calculated Ni–Ni distance for complex **8** (2.284 \AA) is 0.061 \AA shorter than that determined by X-ray measurement.⁶ Nevertheless, the calculations correctly predict the Ni–Ni bond shortening observed for complexes **2**. With respect to **3a**, the optimized Ni–Ni distance of **2a** is 0.061 \AA shorter. For **3a** and **7** the calculations predict

(20) Frisch, M. J.; Trucks, G. W.; Schlegel, H. B.; Gill, P. M. W.; Johnson, B. G.; Robb, M. A.; Cheeseman, J. R.; Keith, T.; Petersson, G. A.; Montgomery, J. A.; Raghavachari, K.; Al-Laham, M. A.; Zakrzewski, V. G.; Ortiz, J. V.; Foresman, J. B.; Cioslowski, J.; Stefanov, B. B.; Nanayakkara, A.; Challacombe, M.; Peng, C. Y.; Ayala, P. Y.; Chen, W.; Wong, M. W.; Andres, J. L.; Replogle, E. S.; Gomperts, R.; Martin, R. L.; Fox, D. J.; Binkley, J. S.; Defrees, D. J.; Baker, J.; Stewart, J. P.; Head-Gordon, M.; Gonzalez, C.; Pople, J. A. *Gaussian 94*, Revision D.2; Gaussian, Inc., Pittsburgh, PA, 1995.

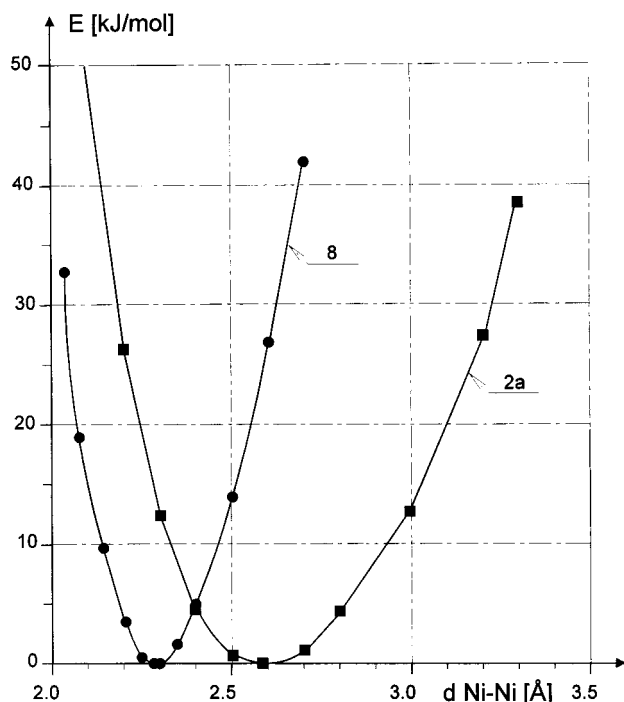
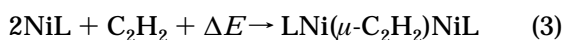


Figure 2. Plots of the calculated total energy versus the Ni–Ni bond lengths of **2a** and **8**.

almost the same Ni–Ni distances of 2.649 and 2.658 Å, respectively. With respect to the corresponding terminal acetylene ligands the optimized C–C bond distance of bridging acetylenes is 0.075 Å (**2a**), 0.062 Å (**3a**), and 0.063 Å (**7**) longer and deviates only slightly from the normal C=C bond length (1.34 Å). This is due to the fact that the bonding of terminal alkynes involves only one π bond and is alkene-like,²¹ whereas the bridging alkyne unit participates with both π bonds in metal–ligand bonding.¹¹

B. Energetics of Stabilizing Interactions in 2a and 8. In Figure 2 we show the plots of the calculated total energy versus the Ni–Ni bond length of **2a** and **8**.

The potential energy curve for the d^9 – d^9 system **8** is steeper than that of the d^{10} – d^{10} system **2a**. In **2a** an elongation or compression of the Ni–Ni equilibrium distance by as much as 0.3 Å causes an energy change by no more than 10 kJ/mol and for **2a** with experimental Ni–Ni bond length we observe only an insignificant increase in energy by 1 kJ/mol. Hence, we propose that if some kind of Ni–Ni bonding is present in **2a**, it should be very soft so that the experimentally observed short Ni–Ni bond distance may presumably result from crystal packing forces. If we build up complex **2a** and **8** from organometallic fragments and an acetylene (eq 3), the energy of this process amounts to –494 kJ/mol for **2a** and –637 kJ/mol for **8**.



Both values account for the binding energy of bridging acetylene and the energy of Ni–Ni bonding. It is interesting to note that the calculated dissociation

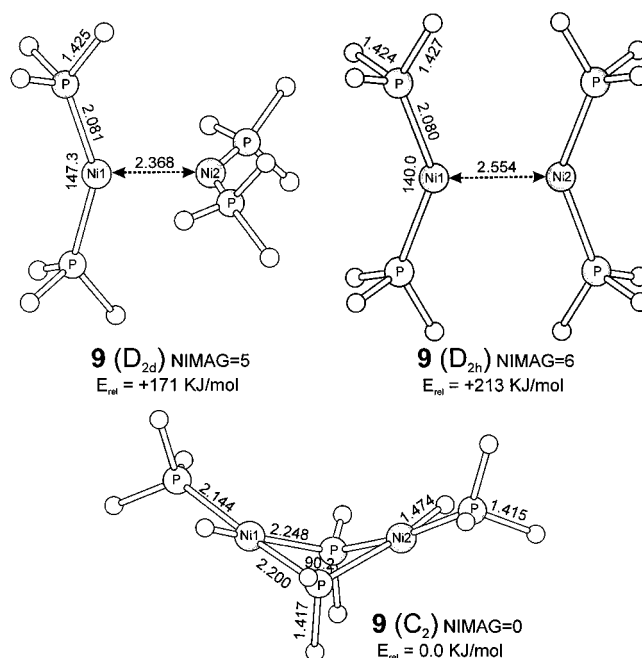


Figure 3. Optimized conformers and number of imaginary frequencies (NIMAG) of the hypothetical molecule $[\text{Ni}(\text{PH}_3)_2]_2$ (**9**). Bond distances are given in Å and bond angles in deg.

energy (CASPT2 level) of the Ni_2 molecule amounts to 202 kJ/mol.²² As can be expected for complex **8**, a single Ni–Ni bond was recognized by the NBO algorithm. In **8** the covalent Ni–Ni bond is constructed from hybrid orbitals having 15% 4s, 2% 4p, and 83% 3d character; the calculated Ni–Ni bond order amounts to 1.035. It is clear that a covalent Ni–Ni interaction is not possible for **2a**, **3a**, and **7**. We notice, however, that by means of extended Hückel calculations it was shown how an admixture of the empty $(n+1)s$ and $(n+1)p$ metal levels into molecular orbitals of the essentially repulsive d^{10} – d^{10} systems diminishes the repulsion and eventually leads to a bonding situation.²³ To investigate the nature of such metal–metal donor–acceptor interactions in **2a**, **3a**, and **7** in the next section, we compare the molecular and electronic structure of the purely hypothetical model complexes $[\text{NiL}_2]_2$ ($\text{L} = \text{PH}_3$ (**9**), $2\text{L} = \text{C}_2\text{H}_2$ (**10**)) with those of acetylene-bridged systems.

C. Ni–Ni Interaction in the Hypothetical Molecules 9 and 10 and in the Corresponding Acetylene-Bridged Systems. The optimized conformers of complexes **9** and **10** are shown in Figures 3 and 4.

Although all conformers are purely hypothetical structures, **9**(D_{2d}) can be related to the platinum complex $[\text{Pt}(t\text{-Bu})_2\text{P}(\text{CH}_2)_3\text{P}(t\text{-Bu})_2]_2$ experimentally observed by Otsuka et al.²⁴ For both types of complexes, the D_{2d} symmetry conformers are more stable than the D_{2h} ones. The Ni–Ni distance in **9**(D_{2d}) (2.368 Å) and **10**(D_{2d}) (2.457 Å) adopts an intermediate value between the 2.248 Å of the single Ni–Ni bond in **8** and the Ni(d^{10})–Ni(d^{10}) distances of 2.588, 2.649, and 2.658 Å in **2a**, **3a**, and **7**, respectively (Figures 1, 3, and 4). We

(21) (a) Rösch, N.; Hoffmann, R. *Inorg. Chem.* **1974**, *13*, 2656. (b) Sakaki, S.; Hari, K.; Ohyoshi, A. *Inorg. Chem.* **1978**, *17*, 3187. (c) Albright, T. A.; Hoffmann, R.; Thibeault, J. C.; Thorn, D. L. *J. Am. Chem. Soc.* **1979**, *101*, 3801. (d) Siegbahn, P. E. M.; Brandemark, U. B. *Theor. Chim. Acta* **1986**, *69*, 119.

(22) Pou-Amerigo, R.; Merchan, M.; Nebot-Gil, I.; Malmqvist, P.-Å.; Roos, B. O. *J. Chem. Phys.* **1994**, *101*, 4893.

(23) (a) Dedieu, A.; Hoffmann, R. *J. Am. Chem. Soc.* **1978**, *100*, 2074. (b) Mehrotra, P. K.; Hoffmann, R. *Inorg. Chem.* **1978**, *17*, 2187.

(24) Yoshida, T.; Yamagata, T.; Tulip, T. H.; Ibers, J. A.; Otsuka, S. *J. Am. Chem. Soc.* **1978**, *100*, 2063.

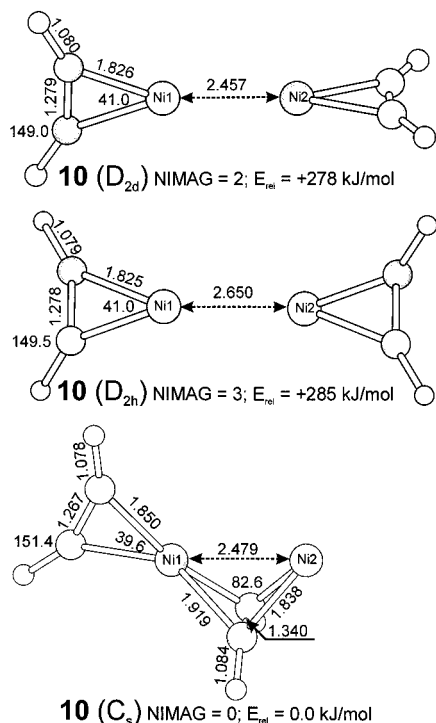
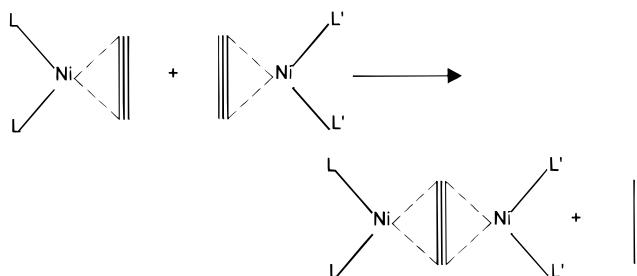


Figure 4. Optimized conformers and number of imaginary frequencies (NIMAG) of the hypothetical molecule $[\text{Ni}(\text{C}_2\text{H}_2)_2]$ (**10**). Bond distances are given in Å and bond angles in deg.

notice, however, that frequency calculations for **9**(D_{2d}) give five imaginary modes (i97.2(a_2), i77.8(e), i28.9(e) cm^{-1}) and for **10**(D_{2d}) two imaginary modes (i267.1(e) cm^{-1}) and consequently both conformers cannot correspond to a minimum on the potential energy surface. If we lower the symmetry constraints during a geometry optimization, **9**(D_{2d}) undergoes P–H cleavage and rearranges to the Ni(II) complex **9**(C_2), displaying terminal hydrido and bridging phosphido ligands (Figure 3, bottom), while **10**(D_{2d}) rearranges to the acetylene-bridged species **10**(C_s) (Figure 4, bottom). With respect to the D_{2d} symmetry conformers, **9**(C_2) and **10**(C_s) are 171 and 278 kJ/mol more stable. Nevertheless, combination of two isolated $\text{Ni}(\text{PH}_3)_2$ or $\text{Ni}(\text{C}_2\text{H}_2)$ fragments to form the dinuclear complexes **9**(D_{2d}) and **10**(D_{2d}) yields energies of 83 kJ/mol (**9**(D_{2d})) and 17 kJ/mol (**10**(D_{2d})), which in the absence of bridging ligands must be attributed to a $\text{Ni}(\text{d}^{10})$ – $\text{Ni}(\text{d}^{10})$ “bond”. It is interesting to note that the experimentally estimated strength of the Au(I)–Au(I) interaction is on the order of 20–50 kJ/mol.⁷ The energies of Au(I)–Au(I) interactions are of the same order of magnitude as those of typical hydrogen bridge bonds.²⁵ The origin of the d^{10} – d^{10} interaction in **9**(D_{2d}) and **10**(D_{2d}) is found by the NBO population analysis in electron density delocalizations from the occupied 3d NBO of one Ni atom into the acceptor 4s NBO of the second Ni atom. The perturbative estimate of the stabilization energy $E_{ij}^{(2)}$ for these donor–acceptor interactions amounts to 156 kJ/mol for **9**(D_{2d}) and 252 kJ/mol for **10**(D_{2d}). The addition of a bridging acetylene to **9**(D_{2d}) and **10**(D_{2d}) to form the complexes $(\text{PH}_3)_2\text{Ni}(\mu\text{-C}_2\text{H}_2)\text{Ni}(\text{PH}_3)_2$ (**11**) and $(\text{C}_2\text{H}_2)\text{-Ni}(\mu\text{-C}_2\text{H}_2)\text{Ni}(\text{C}_2\text{H}_2)$ (**7**) greatly diminishes the strength

(25) Jeffrey, G. A.; Saenger, W. *Hydrogen Bonding in Biological Structures*; Springer: Berlin, 1994.

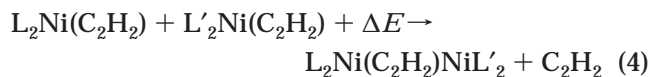
Scheme 1



of Ni–Ni bonding. For **11** and **7** the calculated $E_{ij}^{(2)}$ values amount to 36 and 28 kJ/mol, respectively. These values suggest that in acetylene-bridged species the $\text{Ni}(0)$ – $\text{Ni}(0)$ interaction has to compete against the electronic preferences of the bridging acetylene ligand. Small $E_{ij}^{(2)}$ values are also calculated for **3a** (30 kJ/mol) (Table 2).

In complexes with equivalent nickel atoms such as **3a**, **7**, and **11** the electron density transfer from one nickel atom to the other is the same in both directions. In contrast, in complexes with two dissimilar nickel atoms such as **2a** and **10**(C_s) the transfer of charge from Ni1 to Ni2 is about 3 times greater than that in the reverse direction. This unsymmetrical donor–acceptor relation leads to an increase of the bonding interactions with respect to symmetrical binuclear complexes, and the perturbational interaction energy between the nickel atoms in **2a** (56 kJ/mol) is 2 times greater than that in **7**. The calculated $E_{ij}^{(2)}$ value for **10**(C_s) amounts to 66 kJ/mol. Since in the presence of bridging ligands it is generally not possible to decompose the computed binding energy (eq 3) into a “genuine” ligand component arising exclusively from the interaction of the ligand with both metal centers and the energy of metal–metal bonding, we cannot be sure whether the increase of donor–acceptor interactions between dissimilar nickel atoms corresponds to an increase of Ni–Ni bonding. We have therefore calculated the energetics of condensation reactions (Scheme 1, eq 4) for some combinations of the ligands L and L’.

D. Energetics of the Condensation Reactions. In the condensation reactions from Scheme 1 and eq 4 two terminal acetylenes are replaced by a bridging one.



The calculated energetics of condensation reactions under investigation together with the optimized Ni–Ni distance and the Ni–Ni Wiberg bond indices²⁶ of the products are collected in Table 3. The optimized structures of the condensation products ($\mu\text{-C}_2\text{H}_2$)- $[\text{Ni}(\text{PH}_3)_2]_2$ (**11**), ($\mu\text{-C}_2\text{H}_2$)- $[\text{Ni}(\text{CO})_2]_2$ (**12**), and ($\mu\text{-C}_2\text{H}_2$)- Ni_2 (**13**) are displayed in Figure 5.

According to vibrational analyses all these species represent minima on the potential energy surface. The optimized Ni–Ni distances of complex **11** (2.840 Å) and **12** (2.852 Å) are longer than in the case of **2a**, **3a**, and **7**. The Ni–Ni distance of complex **13** (2.624 Å) lies between those of **2a** (2.587 Å) and **3a** (2.649 Å) or **7** (2.658 Å). Now, we propose an energetic criterion for

(26) Wiberg, K. B. *Tetrahedron* **1968**, *24*, 1083.

Table 2. Second-Order Perturbative Energy $E_{ij}^{(2)}$ (kJ/mol) of Donor–Acceptor Ni–Ni Interactions in the NBO Basis

compd	donor NBO	occ ^a	character		acceptor NBO	occ ^a	character		$E_{ij}^{(2)}$
			% s	% d			% s	% d	
9 (D_{2d})	Lp(1) Ni1	1.969	8	92	Lp* Ni2	0.456	88	12	9
	Lp(2) Ni1	1.820	6	94					69
11	Lp Ni1	1.976	5	95	Lp* Ni2	0.374	96	4	18
10 (D_{2d})	Lp Ni1	1.986	11	89	Lp* Ni2	0.458	79	21	126
	Lp Ni1	1.972	5	95	Lp* Ni2	0.332	93	7	14
3a	Lp Ni1	1.979	7	93	Lp* Ni2/3	0.331	93	7	15
12	Lp. Ni1	1.988	5	95	Lp* Ni2	0.413	96	4	13
2a	Lp Ni1	1.974	6	94	Lp* Ni2	0.313	90	10	15
	Lp Ni2	1.928	6	92	Lp* Ni1	0.356	93	7	41
10 (C_s)	Lp Ni1	1.922	5	95	Lp* Ni2	0.345	83	17	12
	Lp(1) Ni2	1.976	5	86	Lp* Ni1	0.357	93	7	6
	Lp(2) Ni2	1.925	12	88					48
13	Lp(1) Ni1	1.955	14	86	Lp* Ni2	0.437	81	19	9
	Lp(2) Ni1	1.909	5	95					15

^a occ gives the NBO occupancy.

Table 3. Energetics of the Condensation Reactions from Eq 4, Optimized Ni–Ni Distances, and Ni–Ni Wiberg Bond Indices (WBI)²⁶

compd	2L	2L'	ΔE (kJ/mol)	d_{Ni-Ni} (Å)	WBI
3a	Ni(C ₂ H ₂) ₂	C ₂ H ₂	7	2.649	0.102
7	C ₂ H ₂	C ₂ H ₂	9	2.658	0.099
11	2PH ₃	2PH ₃	4	2.840	0.073
12	2CO	2CO	7	2.852	0.046
2a	C ₂ H ₂	2NH ₃	–11	2.587	0.141
10 (C_s)	C ₂ H ₂	none	–7	2.479	0.221
13	none	none	–27	2.624	0.373

defining the existence of an *effective* Ni–Ni d^{10} – d^{10} “bond” based on the assumption that the two coordination sites of the bridging acetylene, i.e., its two π systems, never bind two metal moieties in a synergistic manner. In principle coordination of a Ni(0) moiety to the first π system of acetylene can be assumed to lower, to be indifferent to, or to increase the binding energy of a second Ni(0) moiety to the second π system, corresponding to competitive, independent (uncorrelated), and synergistic interactions between the two coordination sites of acetylene. However, it seems plausible from chemical intuition to assume coordination to the two π systems of acetylene to be *competitive*. A “singly” coordinated acetylene molecule receives a considerable amount of charge from the metal by back-donation.¹¹ It will therefore most likely fall short to an acetylene in its acceptor capacity with respect to a second metal center. Indeed, the combined electron density of terminal acetylenes in the substrates (eq 4, Scheme 1) is always greater than that of bridging acetylene in the corresponding condensation product.¹¹ The energy gained by coordination will to some extent correlate with the charge exchanged, and the energy of the second Ni–acetylene bond will most likely fall short of the first. We therefore assume that the binding energy attributed to a bridging acetylene (BE(C₂H₂)^b) can at most equal (*independent* coordination) but never exceed (*synergistic* coordination) the redoubled value of the binding energy of a terminal acetylene (eq 5).

$$BE(C_2H_2)^b \leq 2BE(C_2H_2)^t \quad (5)$$

Thus, in cases where the overall reaction energy of the condensation process (4) is found to be exothermic, this exothermicity may be regarded as an *effective* stabilizing energy from Ni–Ni bonding. On the basis of

this criterion the data in Table 3 show that Ni–Ni bonding does not *effectively* contribute to the stability of **3a**, **7**, **11**, and **12**, as seen from the endothermicity of the corresponding condensation reactions by 7 kJ/mol (**3a**), 9 kJ/mol (**7**), 4 kJ/mol (**11**), and 7 kJ/mol (**12**). In these cases it can be assumed that some additional driving force must be applied to allow condensation. This conclusion is in accord with the experimental finding that the trinuclear complex **3** is only formed with alkyne ligands containing OH groups capable of forming intramolecular hydrogen bonds. The calculated exothermicities of the condensation reactions 27 kJ/mol (**13**), 11 kJ/mol (**2a**), and 7 kJ/mol (**10**(C_s)) indicate that these dinuclear acetylene complexes are indeed effectively stabilized by Ni–Ni bonding. Thus, for complex **2** these findings suggest that hydrogen bonds are not prerequisite for its stabilization. It is interesting to note that analogous platinum complexes without a stabilizing hydrogen bond network are experimentally known species.^{5c} For **3a**, **7**, **11**, and **12** the optimized Ni–Ni distances range from 2.649 to 2.852 Å and the Ni–Ni Wiberg bond indices range from 0.102 to 0.046 (Table 3). For **2a**, **10**(C_s), and **13** the calculated Wiberg bond indices are greater (0.141–0.373) and the Ni–Ni distances shorter (2.479–2.624 Å). The data in Table 3 show that, with respect to **2a** and **10**(C_s), complex **13**, despite its large Ni–Ni distance, has the largest condensation energy and the largest Wiberg bond index. In section B we showed that in the case of **2a** the compression of the equilibrium Ni–Ni distance by 0.139 Å causes only an insignificant increase in energy by 1 kJ/mol. In the case of complex **13** constrained-geometry optimizations, with a frozen Ni–Ni distance of 2.479 Å and all other parameters relaxed, give an increase in energy of 2.8 kJ/mol and a condensation energy of –24.2 kJ/mol. Furthermore, the equilibrium Ni–Ni distance of complex **13** (2.624 Å) is 0.025–0.228 Å shorter than those of **3a**, **7**, **11**, and **12**. We notice that in the case of gold(I) compounds the metallophilic attraction, in addition to the relativistic effect, was attributed to correlation effects and bond shortenings of 0.008–0.035 Å were assumed as evidence for the presence of the Au(I)–Au(I) attraction.^{8f} In the investigated compounds Ni–Ni donor–acceptor interactions in addition to Ni–ligand interactions break the d^{10} configuration of the nickel atoms and augment the amount of the Ni 4s/

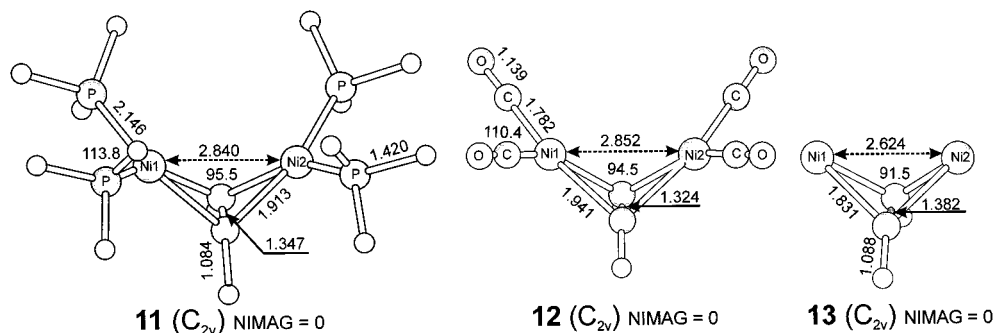


Figure 5. Optimized geometrical parameters and number of imaginary frequencies (NIMAG) of the condensation products **10–13**. Bond distances are given in Å and bond angles in deg.

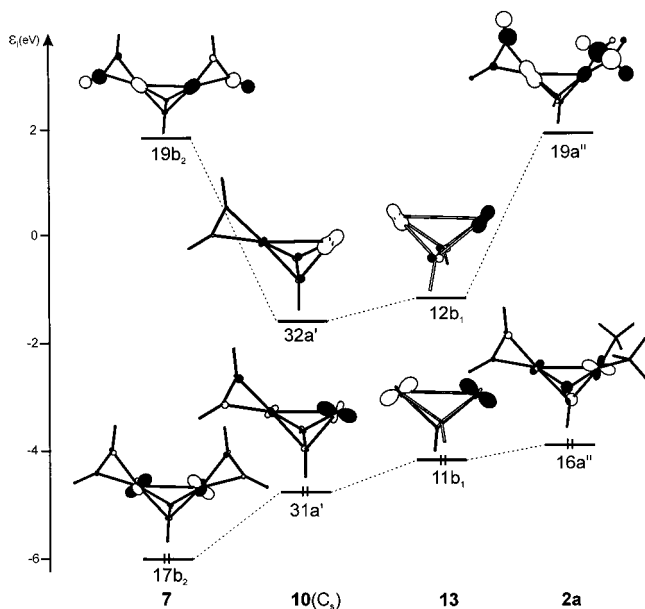


Figure 6. Energy and shape of the HOMOs and of the lowest unoccupied Ni 4s MOs of **7**, **10(C_s)**, **13**, and **2a**.

3d hybridization. The calculated electronic configuration of the Ni atoms in complex **13** is $3d^{8.87}4s^{0.74}$. The population of the Ni1/Ni2 4s levels of **3a**, **7**, **11**, and **12** as well as of the Ni1 4s levels of **2a** and **10(C_s)** is 0.26–0.36e lower. The population of Ni2 4s levels of **2a** and **10(C_s)** is comparable to that in complex **13**. The highest occupied MOs of all investigated compounds are metal-centered levels, mainly composed from Ni 3d AOs. Thus, one can suppose that the degree of the 4s/3d hybridization should be affected by the energetic separation between Ni 3d and 4s MOs. In Figure 6 we present the shapes and energies of the HOMOs and of the lowest empty MOs with predominantly Ni 4s character of **7**, **10(C_s)**, **13**, and **2a**.

It is seen that in **10(C_s)** and **13**, and to some extent in **2a**, the 4s/3d energetic separation is much lower than in the case of complex **7**. We ascribe the closer energetic proximity of nickel 4s and 3d MOs in **10(C_s)**, **13**, and **2a** to the diminished Ni–ligand back-bonding interactions with respect to complex **7**. In the case of gold(I) compounds it was argued that it is the relativistic modification of the gold valence AO energies which brings the 6s and 5d orbitals into close energetic proximity and augments the amount of Au 6s/5d hybridization.^{8a,b}

Conclusion

DFT NBO population analysis indicates that dinuclear Ni(0) complexes without bridging ligands are stabilized due to electron density delocalization from the occupied 3d NBO of one nickel atom into the acceptor 4s NBO of the second nickel atom. The addition of a bridging acetylene greatly diminishes the strength of the Ni(d^{10})–Ni(d^{10}) bonding. For **3a**, **7**, **11**, and **12** the perturbative estimate of the Ni–Ni donor–acceptor stabilization energy (26–36 kJ/mol) is roughly 2 times lower than in the case of **2a**, **10(C_s)**, and **13** (48–66 kJ/mol). The Ni–Ni donor–acceptor interactions in addition to the nickel–ligand interactions break the d^{10} configuration of the nickel atoms and lead to 4s/3d hybridization. The amount of the 4s/3d hybridization correlates with the energetic separation between Ni 3d and 4s MOs, which for **2a**, **10(C_s)**, and **13** is smaller than in the case of **3a**, **7**, **11**, and **12**. We ascribe the closer energetic proximity of Ni 4s and 3d MOs to diminished metal–ligand back-bonding interactions, which in turn destabilize the Ni 3d MOs. The condensation reactions from eq 4 are endothermic for **3a**, **7**, **11**, and **12** and exothermic for **2a**, **10(C_s)**, and **13**. All the above findings suggest that only the latter class of compounds is effectively stabilized by Ni–Ni bonding. The formation of homoleptic complexes $M_n(RC\equiv CR)_{n+1}$ of d^{10} metals needs an additional driving force and should be facilitated in cases where alkyne ligands are capable of forming intra- or intermolecular hydrogen bonds. As mentioned previously, the energy of hydrogen bonding is of the same order of magnitude as the experimentally known estimates of the d^{10} – d^{10} bond strength. Hydrogen bonds are not prerequisites for the stabilization of **10(C_s)**, **13**, and complexes of type **2**. Due to structural and electronic preferences of the bridging acetylene ligand, the potential energy surface around the equilibrium Ni–Ni distance of the investigated compounds is flat and consequently Ni(0)–Ni(0) interactions should be characterized as weak interactions, similar to the case of Au(I)–Au(I) bonds.

Acknowledgment. Our work was supported by BMFT Project “Katalysis” as well as the Schwerpunkt “Katalyse” of the State of Baden-Württemberg. Further support was given by the Deutsche Forschungsgemeinschaft (SFB 247) and the Fonds der Chemischen Industrie.

OM990277B